

AN ANALYTICAL METHOD TO DETERMINE SCOUR

Dr.ir. S.A. Miedema¹

ABSTRACT

The loading process of TSHD's (Trailing Suction Hopper Dredgers) is often terminated because of the occurrence of scour/erosion of the just settled sand. If the flow velocity above the sediment is too high, scour will occur and the sand particles will not settle anymore. But when does this occur?, and what is the relation between the scour velocity and the sedimentation process? In the 30's Shields discovered a relation between the particle Reynolds number and the shear stress, the well known Shields curve. Hjulstrøm also discovered a similar relation, but directly between the flow velocity and the particle diameter.

In the paper a relation is derived between the relevant grain parameters and the operational parameters, resulting in curves that can be plotted both in the Shields and the Hjulstrøm approach. Based on the geometry of the grain with respect to the sediment, different curves can be constructed for different cases of scour, from a single grain being eroded to the entire top layer being eroded. The "new" theory is added to the existing Camp, Miedema & Vlasblom model for Hopper Sedimentation, however it can also be used in any morphological problem.

INTRODUCTION

During the final phase of the loading cycle the sediment level in the hopper is rising due to sedimentation, the flow velocity above the sediment increases, resulting in scour. This is the cause of rapidly increasing overflow losses. Figure 1 shows this situation. From literature a number of approaches can be found, the Camp approach for sedimentation tanks and the Shields and Hjulstrøm approaches for erosion in rivers. In general erosion is defined as the pickup of particles because of the flow of water above the particles. During the final phase of the loading cycle of a TSHD however, there is a high density mixture flowing above the bed and not just water. This may influence the way and the moment scour occurs. To find a solution to this problem, the physics of erosion will be analyzed.

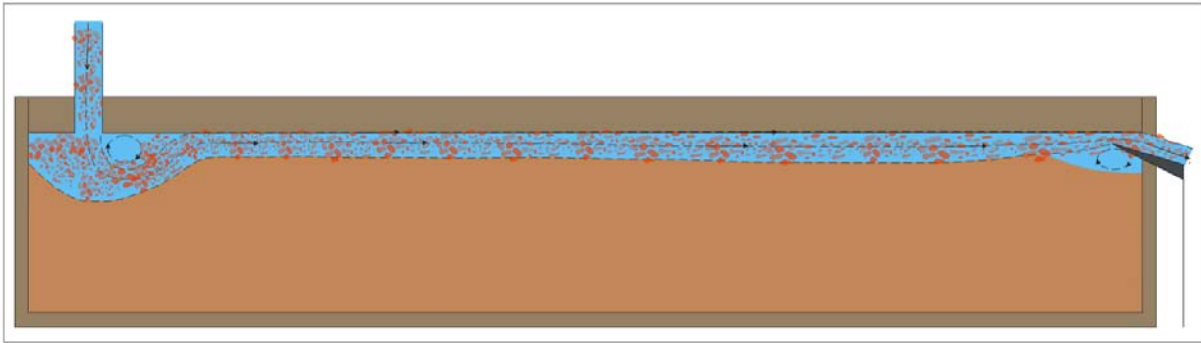


Figure 1. The final phase of the loading cycle.

THE CAMP APPROACH

When the height of the sediment increases and the hopper load parameter remains constant, the horizontal flow velocity above the sediment also increases. Grains that have already settled will be re-suspended and leave the basin through the overflow. This is called scouring. First the small grains will not settle or erode and when the level increases more, also the bigger grains will stop settling, resulting in a smaller settling efficiency. The shear force of water on a spherical particle is:

$$\tau = \frac{1}{4} \cdot \lambda \cdot \frac{1}{2} \cdot \rho_w \cdot s_s^2 \quad (1)$$

¹ Delft University of Technology, Faculty 3mE, The Netherlands. s.a.miedema@3me.tudelft.nl

The shear force of particles at the bottom (mechanical friction) is proportional to the submerged weight of the sludge layer, per unit of bed surface (see Figure 2):

$$f = \mu \cdot N = \mu \cdot (1-n) \cdot (\rho_q - \rho_w) \cdot g \cdot d \quad (2)$$

In equilibrium the hydraulic shear equals the mechanical shear and the critical scour velocity can be calculated. The scour s_s velocity for a specific grain with diameter d_s , according to Huisman (1995) and Camp (1946) is:

$$s_s = \sqrt{\frac{8 \cdot \mu \cdot (1-n) \cdot (\rho_q - \rho_w) \cdot g \cdot d_s}{\lambda \cdot \rho_w}} \quad (3)$$

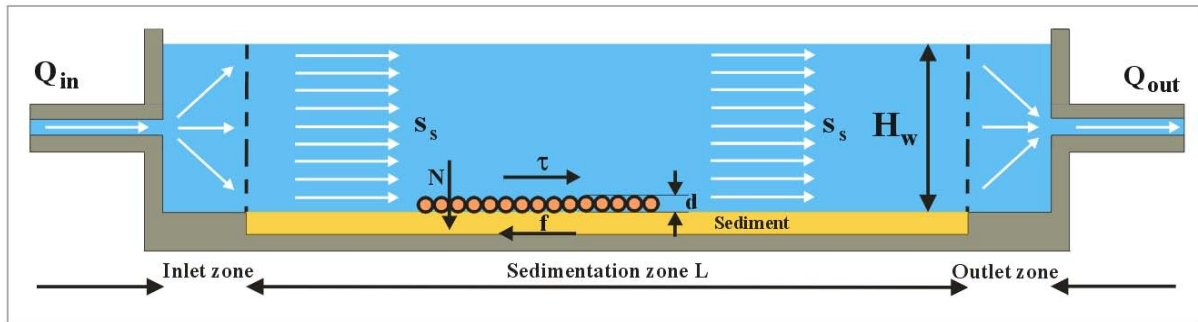


Figure 2. The equilibrium of forces on a particle.

Grains that are re suspended due to scour, will not stay in the basin and thus have a settling efficiency of zero. In this equation, λ is the viscous friction coefficient mobilized on the top surface of the sediment and has a value in the range of 0.01-0.03, depending upon the Reynolds number and the ratio between the hydraulic radius and the grain size (surface roughness). The porosity n has a value in the range 0.4-0.5, while the friction coefficient μ depends on the internal friction of the sediment and has a value in the range of 0.1-1.0 for sand grains. With $\mu \cdot (1-n) = 0.05$ and $\lambda = 0.03$ this gives:

$$s_s = \sqrt{\frac{40 \cdot (\rho_q - \rho_w) \cdot g \cdot d_s}{3 \cdot \rho_w}} \quad (4)$$

The particle diameter of particles that will not settle due to scour (and all particles with a smaller diameter) is:

$$d_s = \frac{3 \cdot \rho_w}{40 \cdot (\rho_q - \rho_w) \cdot g} \cdot s_s^2 \quad (5)$$

Knowing the diameter d_s , the fraction p_s that will not settle due to scour can be found if the PSD of the sand is known. Equation 4 is often used for designing settling basins for drinking water. In such basins scour should be avoided, resulting in an equation with a safety margin. For the prediction of the erosion during the final phase of the settling process in TSHD's a more accurate prediction of the scour velocity is required.

THE SHIELDS APPROACH

Let us consider the steady flow over the bed composed of cohesion less grains. The forces acting on the grain are shown in Figure 3. The driving force is the flow drag force on the grain, assuming that part of the surface of the particle is hiding behind other particles and only a fraction β is subject to drag and lift:

$$F_D = C_D \cdot \frac{1}{2} \cdot \rho_w \cdot (\alpha \cdot u_*^2) \cdot \beta \cdot \frac{\pi \cdot d^2}{4} \quad (6)$$

The lift force is written in the same way:

$$F_L = C_L \cdot \frac{1}{2} \cdot \rho_w \cdot (\alpha \cdot u_*^*)^2 \cdot \beta \cdot \frac{\pi \cdot d^2}{4} \quad (7)$$

The submerged weight of the particle is:

$$F_w = (\rho_q - \rho_w) \cdot g \cdot \frac{\pi \cdot d^3}{6} \quad (8)$$

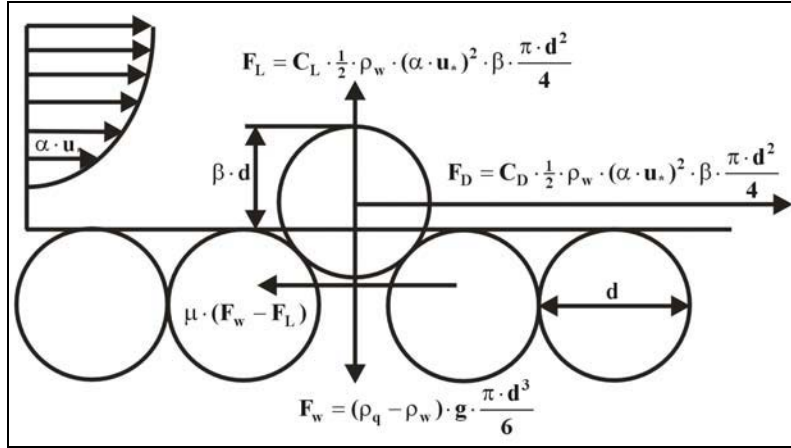


Figure 3. Forces acting on a grain resting on the bed.

At equilibrium:

$$F_D = \mu \cdot (F_w - F_L) \quad (9)$$

where the friction velocity u_* is the flow velocity close to the bed. α is a coefficient, used to modify u_* so that αu_* forms the characteristic flow velocity past the grain. The stabilizing force can be modeled as the friction force acting on the grain. If $u_{*,c}$, critical friction velocity, denotes the situation where the grain is about to move, then the drag force is equal to the friction force, so:

$$C_D \cdot \frac{1}{2} \cdot \rho_w \cdot (\alpha \cdot u_{*,c})^2 \cdot \beta \cdot \frac{\pi \cdot d^2}{4} = \mu \cdot \left((\rho_q - \rho_w) \cdot g \cdot \frac{\pi \cdot d^3}{6} - C_L \cdot \frac{1}{2} \cdot \rho_w \cdot (\alpha \cdot u_{*,c})^2 \cdot \beta \cdot \frac{\pi \cdot d^2}{4} \right) \quad (10)$$

Which can be re-arranged into:

$$\frac{u_{*,c}^2}{R_d \cdot g \cdot d} = \frac{4}{3} \cdot \frac{1}{\alpha^2} \cdot \frac{\mu}{\beta \cdot C_D + \mu \cdot \beta \cdot C_L} \quad (11)$$

The Shields parameter is now defined as:

$$\theta_c = \frac{u_{*,c}^2}{R_d \cdot g \cdot d} \quad (12)$$

Re-arranging gives a simple equation for the Shields parameter:

$$\theta_c = \frac{u_{*,c}^2}{R_d \cdot g \cdot d} = \frac{4}{3} \cdot \frac{\mu}{\beta} \cdot \frac{1}{\alpha^2} \cdot \frac{1}{C_D + \mu \cdot C_L} \quad (13)$$

Since C_D normally depends on the boundary Reynolds number Re_* , the Shields θ_c number will be a function of the boundary Reynolds number $Re_* = u_* \cdot d/v$. Carrying out an equilibrium of moments around the contact point of a particle with the particle its resting on, results in the same equation. One can discuss which equation to use for the C_D value and the C_L value, since the particles are not free from the surface as with the determination of the settling velocity for individual particles. Now the question is, what would such a function look like. Figure 4 shows the relation between the Shields parameter and the boundary Reynolds number as is shown in Shields (1936).

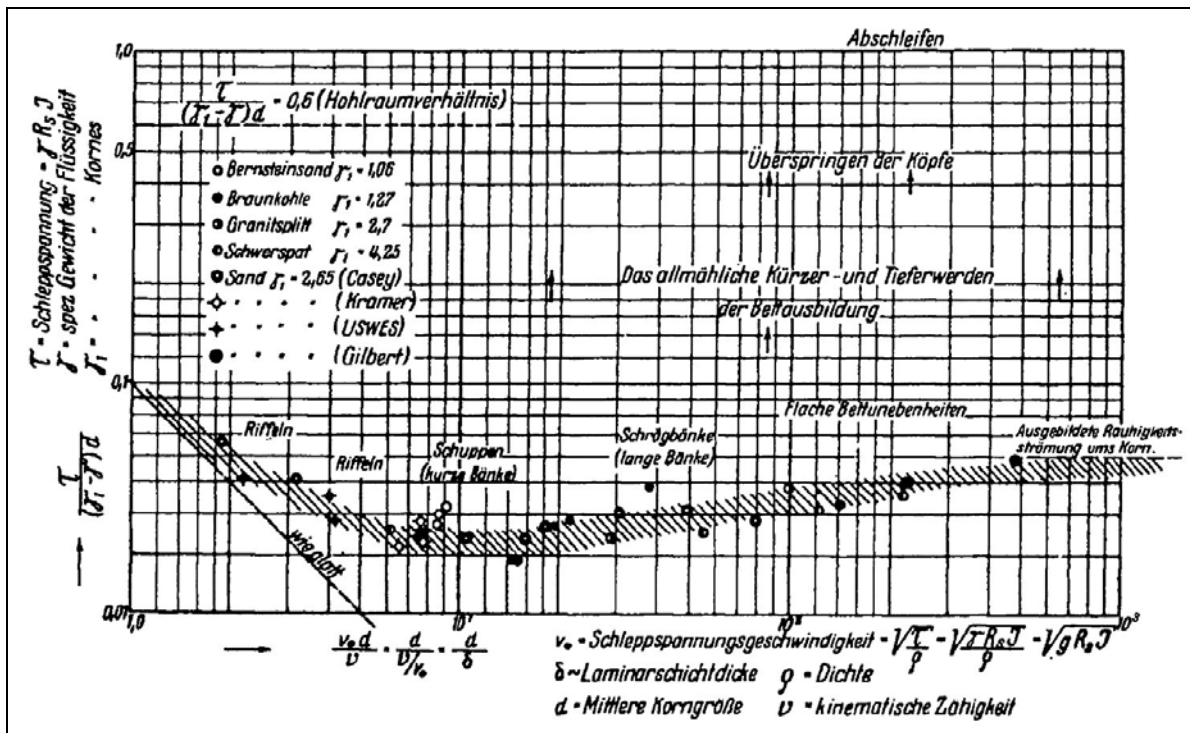


Figure 4. The original Shields (1936) curve.

It is however interesting to investigate if this curve can be determined in a more fundamental way. Based on the theory in this chapter the following can be derived.

Case 1: Hydraulically smooth flow (very low Re_*).

First lets assume a very small particle in a viscous laminar boundary layer. The particle is hiding for $(1 - \beta)$ behind other particles, which also means that β of the surface is subject to drag, assume β is about 0.5, which means the changes in drag area are about proportional with β . The velocity $u(z)$ in the viscous sub layer at β times the diameter d height is equal to:

$$u(\beta \cdot d) = \frac{u_*^2}{\nu} \cdot \beta \cdot d \quad (14)$$

Since the velocity develops linear with z , the drag force exerted on the particle, has to be found by integration of the velocity squared over the surface that is subject to the drag, but since the shape of the particle is not a square, but irregular, an effective velocity of $\frac{1}{3} \cdot \sqrt{3} = 0.577$ of the velocity at the top of the particle is chosen. This gives for the effective velocity on the particle:

$$\mathbf{u}_{\text{eff}} = \frac{1}{3} \cdot \sqrt{3} \cdot \mathbf{u}(\boldsymbol{\beta} \cdot \mathbf{d}) = \frac{1}{3} \cdot \sqrt{3} \cdot \frac{\mathbf{u}_*^2}{\mathbf{v}} \cdot \boldsymbol{\beta} \cdot \mathbf{d} = \frac{1}{3} \cdot \sqrt{3} \cdot \boldsymbol{\beta} \cdot \frac{\mathbf{u}_*^2}{\mathbf{v}} \cdot \mathbf{d} \quad (15)$$

With:

$$\mathbf{u}_{\text{eff}} = \boldsymbol{\alpha} \cdot \mathbf{u}_* = \frac{1}{3} \cdot \sqrt{3} \cdot \boldsymbol{\beta} \cdot \frac{\mathbf{u}_*}{\mathbf{v}} \cdot \mathbf{d} \cdot \mathbf{u}_* \quad (16)$$

So the coefficient $\boldsymbol{\alpha}$ is equal to:

$$\boldsymbol{\alpha} = \frac{1}{3} \cdot \sqrt{3} \cdot \boldsymbol{\beta} \cdot \frac{\mathbf{u}_*}{\mathbf{v}} \cdot \mathbf{d} = \frac{1}{3} \cdot \sqrt{3} \cdot \boldsymbol{\beta} \cdot \mathbf{Re}_* \quad (17)$$

The Reynolds number for the flow around the particle is, assuming the hydraulic diameter of the particle equals 4 times the area that is subject to drag, divided by the wetted perimeter equals \mathbf{d} :

$$\mathbf{Re}_p = \frac{\mathbf{u}_{\text{eff}} \cdot \mathbf{d}}{\mathbf{v}} = \frac{1}{3} \cdot \sqrt{3} \cdot \boldsymbol{\beta} \cdot \left(\frac{\mathbf{u}_* \cdot \mathbf{d}}{\mathbf{v}} \right)^2 = \frac{1}{3} \cdot \sqrt{3} \cdot \boldsymbol{\beta} \cdot \mathbf{Re}_*^2 = \boldsymbol{\alpha} \cdot \mathbf{Re}_* \quad (18)$$

The drag coefficient in this Stokes area equals, as already mentioned in chapter 4.:

$$C_D = \frac{24}{\mathbf{Re}_p} \quad (19)$$

Substituting this in equation 13 gives for the Shields parameter:

$$\theta_c = \frac{4}{3} \cdot \frac{\boldsymbol{\mu}}{\boldsymbol{\beta}} \cdot \left(\frac{1}{\frac{1}{3} \cdot \sqrt{3} \cdot \boldsymbol{\beta} \cdot \mathbf{Re}_*} \right)^2 \cdot \frac{\frac{1}{3} \cdot \sqrt{3} \cdot \boldsymbol{\beta} \cdot \mathbf{Re}_*^2}{24} = \frac{\sqrt{3}}{18} \cdot \frac{\boldsymbol{\mu}}{\boldsymbol{\beta}^2} \quad (20)$$

Let's assume a mechanical friction coefficient of $\boldsymbol{\mu}=0.5$ and a surface factor $\boldsymbol{\beta}=0.5$ (meaning that 50% of the particle is subject to drag). This would give a Shields parameter of 0.19. Soulsby & Whitehouse (1997) assume there is a maximum of 0.3, but as can be concluded from equation 20, there must be a certain bandwidth depending on the mechanical friction coefficient $\boldsymbol{\mu}$ and the fraction of the surface of the particle that is subject to drag $\boldsymbol{\beta}$. Using the transition region for C_D , gives:

$$\theta_c = \frac{4}{3} \cdot \frac{\boldsymbol{\mu}}{\boldsymbol{\beta}} \cdot \left(\frac{1}{\frac{1}{3} \cdot \sqrt{3} \cdot \boldsymbol{\beta} \cdot \mathbf{Re}_*} \right)^2 \cdot \frac{1}{\frac{24}{\frac{1}{3} \cdot \sqrt{3} \cdot \boldsymbol{\beta} \cdot \mathbf{Re}_*^2} + \frac{3}{\left(\frac{1}{3} \cdot \sqrt{3} \cdot \boldsymbol{\beta} \cdot \mathbf{Re}_*^2 \right)^{0.5}} + 0.34} \quad (21)$$

Case 2: Hydraulically rough flow (very high \mathbf{Re}_).*

Now let's consider a very course particle in turbulent flow. The velocity equals to:

$$\mathbf{u}(z) = \frac{\mathbf{u}_*}{\boldsymbol{\kappa}} \cdot \ln \left(\frac{z}{0.033 \cdot \mathbf{k}_s} \right) \quad (22)$$

Assuming a roughness \mathbf{k}_s about equal to $\boldsymbol{\beta}$ times the particle diameter \mathbf{d} , gives:

$$\mathbf{u}(\beta \cdot \mathbf{d}) = \frac{\mathbf{u}_*}{\kappa} \cdot \ln\left(\frac{1}{0.033}\right) = 8.53 \cdot \mathbf{u}_* \quad (23)$$

The effective velocity will be smaller, but since the particle is subject to turbulent flow in a logarithmic velocity field, equation 22 should be used to determine the effective velocity the part of the particle subject to drag, with respect to drag. For a logarithmic velocity field this is 0.764 times the velocity at the top of the particle, giving a velocity coefficient $\alpha=6.5$, resulting in an effective velocity of:

$$\mathbf{u}_{\text{eff}} = 6.5 \cdot \mathbf{u}_* \quad (24)$$

And a particle Reynolds number of:

$$\mathbf{Re}_p = \frac{\mathbf{u}_{\text{eff}} \cdot \mathbf{d}}{\nu} = 6.5 \cdot \frac{\mathbf{u}_* \cdot \mathbf{d}}{\nu} = 6.5 \cdot \mathbf{Re}_* = \alpha \cdot \mathbf{Re}_* \quad (25)$$

The drag coefficient C_D has a constant value of 0.445 for turbulent flow. Substituting this in equation 13 gives:

$$\theta_c = \frac{4}{3} \cdot \frac{\mu}{\beta} \cdot \frac{1}{6.5^2} \cdot \frac{1}{0.445} = 0.0709 \cdot \frac{\mu}{\beta} \quad (26)$$

If the mechanical friction coefficient μ and the area coefficient β are chosen equal, this results in a Shields parameter θ_c of about 0.071 for the very high Reynolds \mathbf{Re}_* numbers. In literature a value of 0.055-0.060 is found, but measurements show a certain bandwidth. Using a mechanical friction coefficient μ of 0.45 and an area factor β of 0.55, results in a Shields parameter θ_c of 0.058, which matches literature. Values smaller than 0.5 for the area factor β are unlikely, because the Shields parameters predicts the beginning of erosion/scour of the entire sediment and there will always be particles with a higher area factor β up to about 0.75. Using this maximum area factor with a mechanical friction coefficient μ of 0.45, gives a Shields parameter θ_c of about 0.0425. Using the transition region, gives:

$$\theta_c = \frac{4}{3} \cdot \frac{\mu}{\beta} \cdot \left(\frac{1}{6.5}\right)^2 \cdot \frac{1}{\frac{24}{(6.5 \cdot \mathbf{Re}_*)} + \frac{3}{(6.5 \cdot \mathbf{Re}_*)^{0.5}} + 0.34} \quad (27)$$

Case 3: Transitional flow (medium \mathbf{Re}_).*

In the transitional area, both the linear velocity profile of the viscous sub layer and the logarithmic profile play a role in the forces on a particle. The transitional area has no fixed boundaries, but roughly it's from $\mathbf{Re}_*=0.5$ to $\mathbf{Re}_*=20$. For the transitional area an empirical equation can be used for the velocity profile, according to:

$$\begin{aligned} \alpha &= \mathbf{A} - \mathbf{B} \cdot e^{-\mathbf{C} \cdot \mathbf{Re}_*^{\mathbf{D}}} \\ \mathbf{A} &= 5.62 + 0.70 \cdot \beta \\ \mathbf{B} &= 5.62 + 0.68 \cdot \beta \\ \mathbf{C} &= 0.063 - 0.0237 \cdot \beta \\ \mathbf{D} &= 1.488 - 0.1183 \cdot \beta \end{aligned} \quad (28)$$

With:

$$\mathbf{Re}_p = \alpha \cdot \mathbf{Re}_* \quad (29)$$

Equation 28 has been derived in such a way that the resulting curves match the data measured by Julien (1995) as is shown in Figure 6. Using the transition region for C_D , and equation 13, the Shields curve can be determined. Figure 5 shows the estimated curves for values of β of 0.475, 0.525, 0.6, 0.7, 0.8, 0.9 and 1.0, with in the background the original Shields curve, while Figure 6 shows these, with in the background measured values of the Shields parameter from Julien (1995). The estimated curves are calculated with a friction coefficient $\mu=0.45$ and a lift coefficient $C_L=0.25$. It is very well possible that in reality this coefficient may have a higher value. It is also possible that this coefficient depends on the particle diameter or the particle Reynolds number.

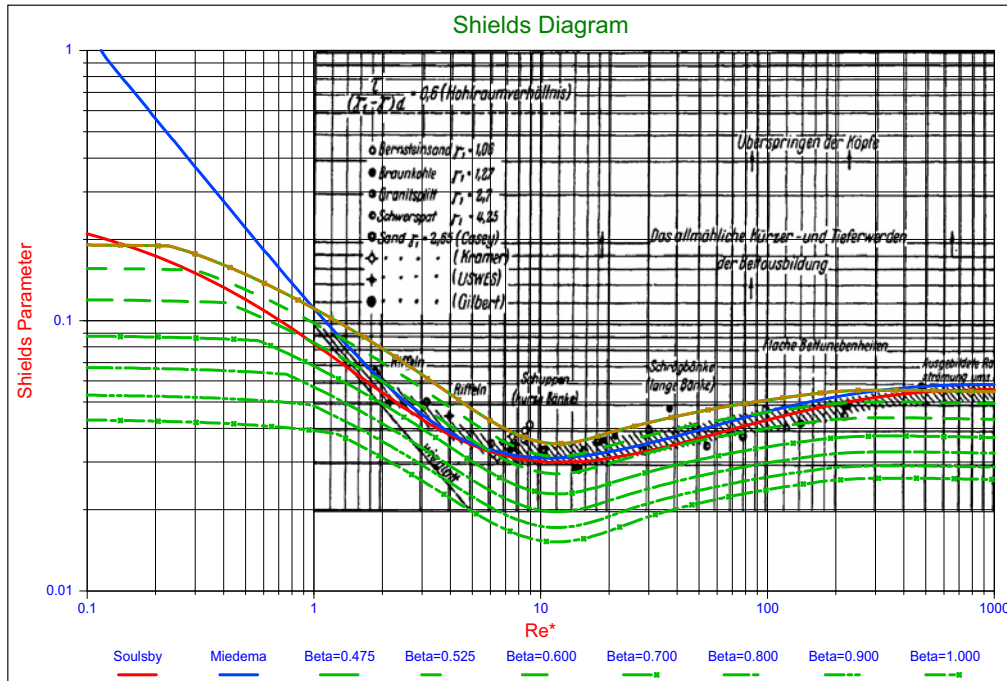


Figure 5. The estimated Shields curves versus the original Shields curve.

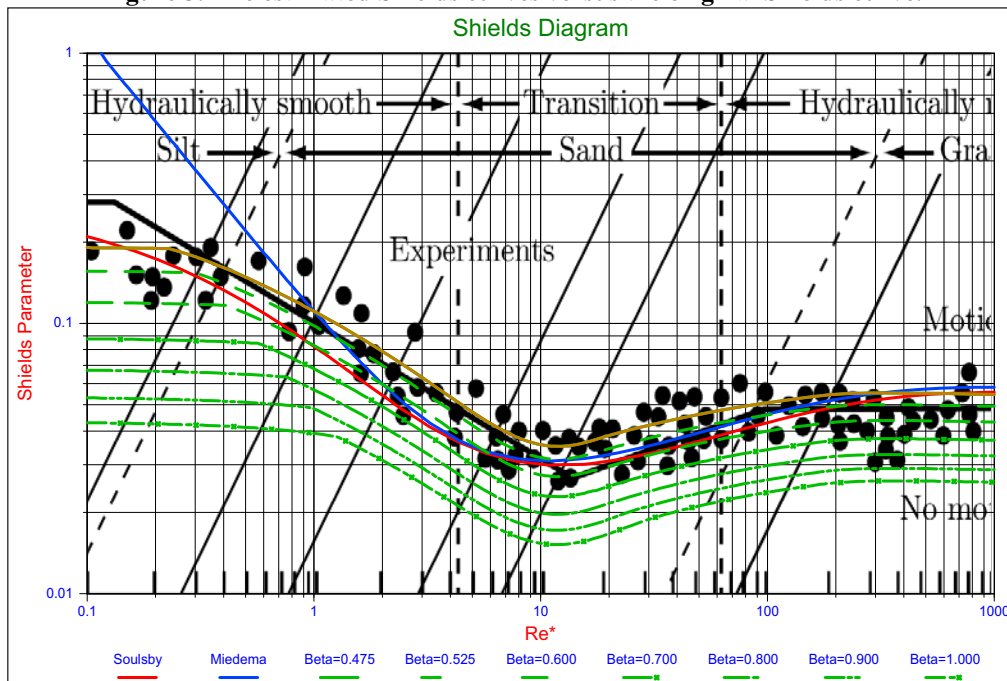


Figure 6. The estimated Shields curves for different values of β .

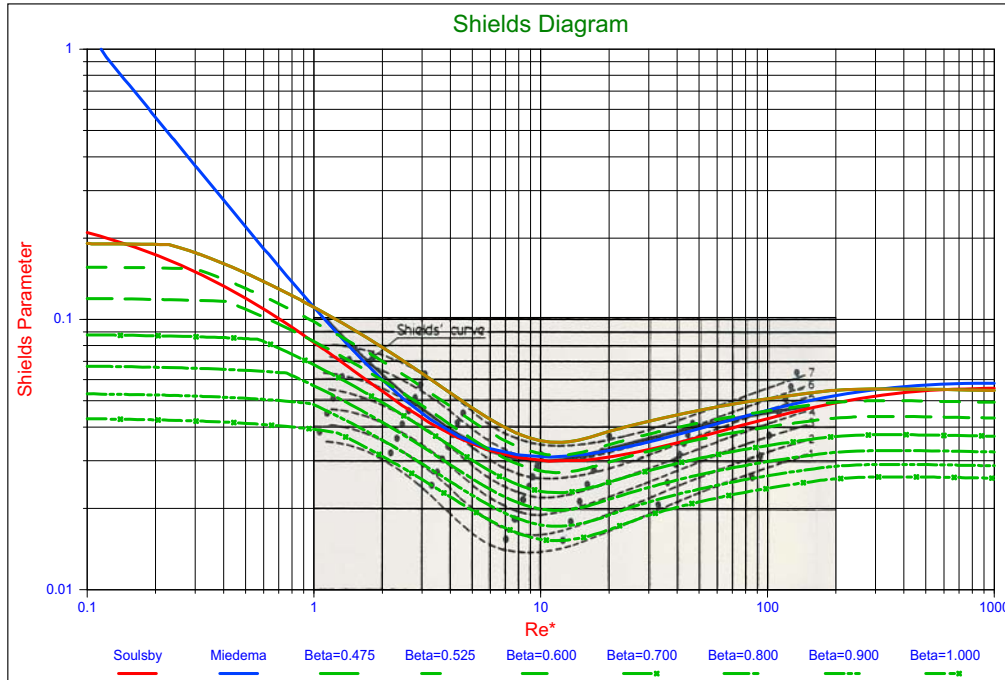


Figure 7. The 7 levels of erosion according to Delft Hydraulics, Breusers (1972).

The Delft Hydraulics, Breusers (1972) defined 7 levels of erosion according to:

1. Occasional particle movement at some locations.
2. Frequent particle movement at some locations.
3. Frequent particle movement at many locations.
4. Frequent particle movement at nearly all locations.
5. Frequent particle movement at all locations.
6. Permanent particle movement at all locations.
7. General transport (initiation of ripples).

As can be seen from Figure 7, the curves with the 7 values for β match closely with the 7 levels according to Delft Hydraulics, Breusers (1972), although there are differences. Since the factor β is the fraction of a particle that is subject to drag, this seems plausible. In a normal sediment, there will be a few particles that lay on top of the bed and that are subject to drag for 100%. These particles will be the first to move (erode), so this is level 1. Particles that are embedded for 50% will be much harder to move and form level 5 or higher.

SIELDS APPROXIMATION EQUATIONS

Many researchers created equations to approximate the Shields curve. The original Shields graph however is not convenient to use, because both axis contain the shear velocity u_* and this is usually an unknown, this makes the graph an implicit graph. To make the graph explicit, the graph has to be transformed to another axis system. In literature often the dimensionless grain diameter D_* is used. This dimensionless diameter also called the Bonnevillie parameter is:

$$D_* = d \cdot \sqrt[3]{\frac{R_d \cdot g}{\nu^2}} \quad (30)$$

With the normal values for the water density, the relative density and the viscosity, the dimensionless diameter is about 20.000 times the particle diameter, or 20 times the particle diameter in mm. Figure 8 & Figure 9 show the Shields approximations of van Rijn (1993), Brownlie (1981), Zanke (2003), Soulsby & Whitehouse (1997) completed with a lower limit, upper limit and average approximation derived for these lecture notes by the author. It is interesting to see that the van Rijn and Brownlie equations result in a continuously increasing Shields parameter

with a decreasing dimensionless diameter, the Zanke (2003) approach does this also, but less steep, while the Soulsby & Whitehouse (1997) approach has a limit of 0.3 for very small particles, matching the model as described in the previous chapter. Only Soulsby & Whitehouse (1997) take the linear velocity profile in the viscous sub layer, resulting in a constant Shields parameter at very low Reynolds numbers, into account.

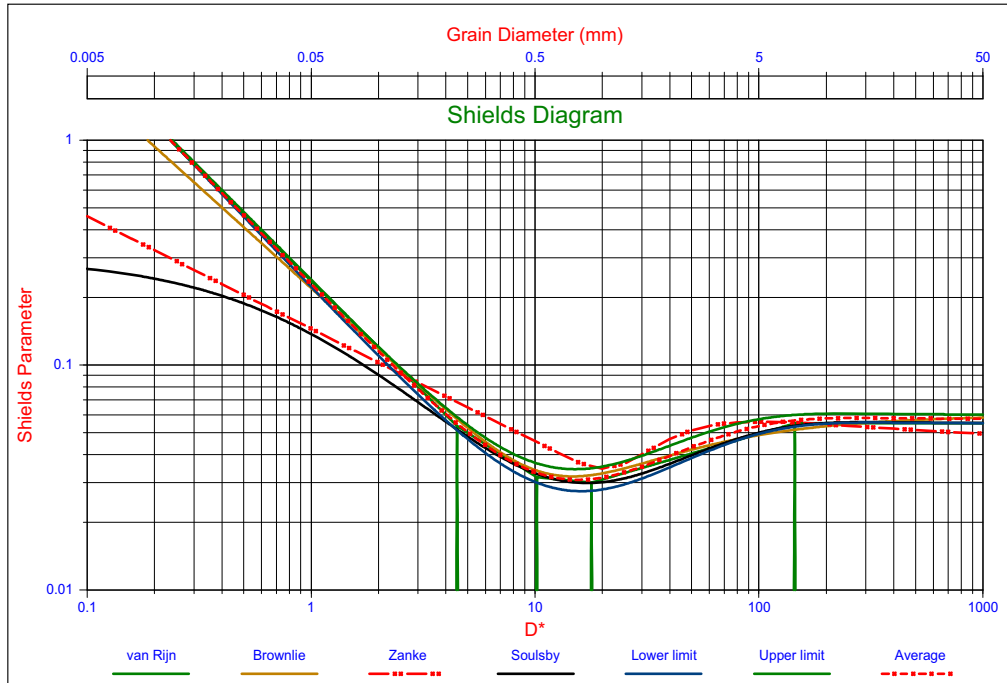


Figure 8. The Shields parameter as a function of the dimensionless diameter.

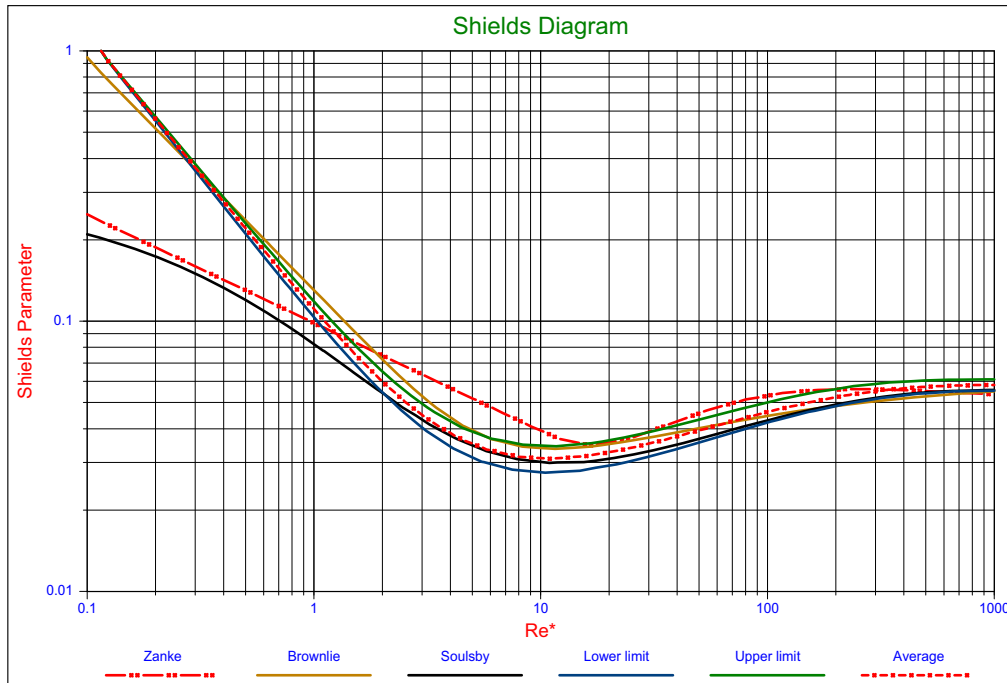


Figure 9. The Shields parameter as a function of the boundary Reynolds number.

From the definition of the Shields parameter, the relation between the Shields parameter and the Bonneville parameter can be derived, the Shields parameter is:

$$\theta_{cr} = \frac{u_*^2}{R_d \cdot g \cdot d} \quad (31)$$

The grain Reynolds number Re_* , which defines the transition between hydraulic smooth and rough conditions for which grains protrude into the flow above the laminar sub layer δ at $Re^*=11.63$ as:

$$Re_* = \frac{u_* \cdot d}{\nu} = \frac{\sqrt{\theta} \cdot \sqrt{R_d \cdot g \cdot d} \cdot d}{\nu} \quad (32)$$

Using equation 30, this gives:

$$Re_* = \sqrt{\theta} \cdot D_*^{1.5} \quad (33)$$

So the Bonneville parameter is a function of the Shields number and the boundary Reynolds number according to:

$$D_* = \left(\frac{Re_*}{\sqrt{\theta}} \right)^{2/3} \quad (34)$$

Another parameter that is often used for the horizontal axis is the so called Grant and Madsen (1976) parameter or sediment fluid parameter, see Figure 10:

$$S_* = \frac{\sqrt{R_d \cdot g \cdot d} \cdot d}{4 \cdot \nu} = \frac{D_*^{1.5}}{4} = \frac{Re_*}{4 \cdot \sqrt{\theta}} \quad (35)$$

The factor of 4 appears in the definition of S_* to render the numerical values of S_* comparable with the Re_* values in the traditional Shields diagram. This is done merely for convenience and has no physical significance.

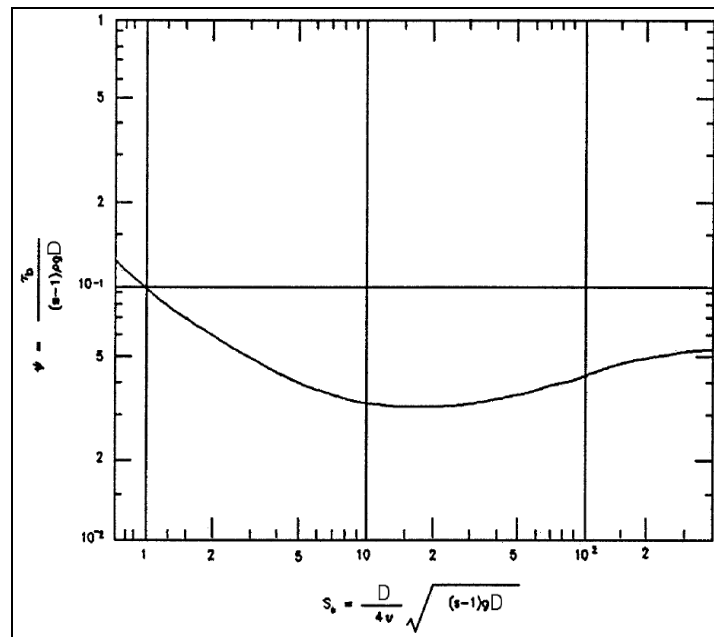


Figure 10. Modified Shields diagram, Madsen & Grant (1976).

Which differs a factor 4 from the particle Reynolds number Re_p :

$$Re_p = \frac{\sqrt{R_d \cdot g \cdot d} \cdot d}{\nu} = D_*^{1.5} = \frac{Re_*}{\sqrt{\theta}} \quad (36)$$

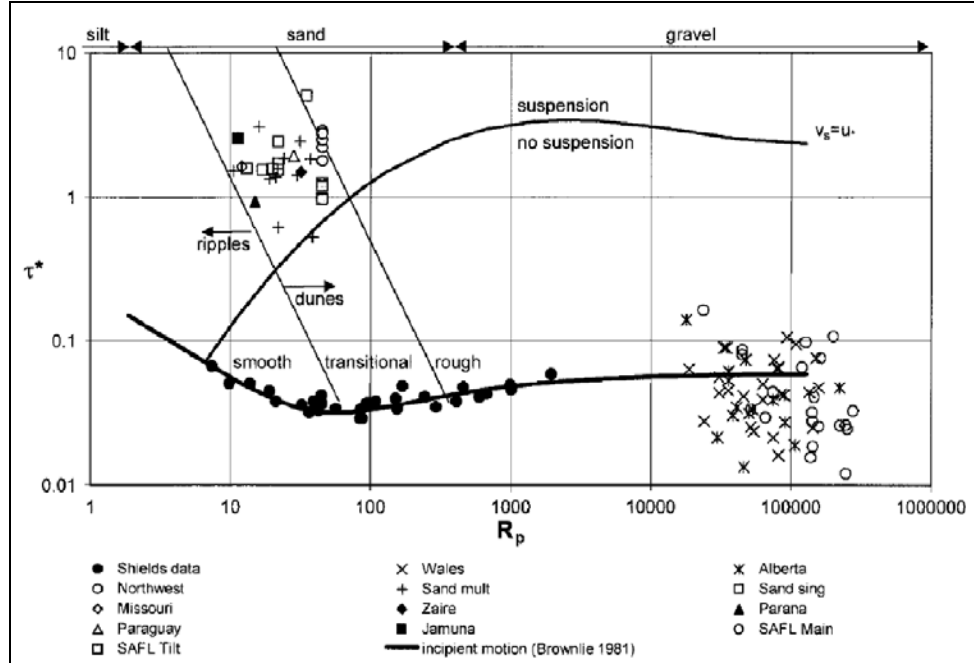


Figure 11. Modified Shields diagram using Re_p (equation 36).

Figure 12 shows the relation between the boundary or grain Reynolds number, the Bonneville parameter (dimensionless grain diameter) and the Grant & Madsen parameter.

The different approximation equations are summarized below.

$$\theta_{cr} = \frac{0.30}{(1 + 1.2 \cdot D_*)} + 0.055 \cdot (1 - e^{-0.02 \cdot D_*}) \quad \text{Soulsby \& Whitehouse} \quad (37)$$

$$\theta_{cr} = \frac{0.22}{D_*^{0.9}} + 0.06 \cdot 10^{-7.7 \cdot D_*^{-0.9}} \quad \text{Brownlie} \quad (38)$$

$$\begin{aligned} \theta_{cr} &= \frac{0.24}{D_*} & D_* < 4.5 \\ \theta_{cr} &= \frac{0.14}{D_*^{0.64}} & 4.5 < D_* < 10.2 \\ \theta_{cr} &= \frac{0.04}{D_*^{0.1}} & 10.2 < D_* < 17.9 \\ \theta_{cr} &= 0.013 \cdot D_*^{0.29} & 17.9 < D_* < 145 \\ \theta_{cr} &= 0.055 & 145 < D_* \end{aligned} \quad \text{van Rijn} \quad (39)$$

$$\theta_{cr} = \frac{0.145}{D_*^{0.5}} + 0.045 \cdot 10^{-1100 \cdot D_*^{-2.25}} \quad \text{Zanke} \quad (40)$$

$$\theta_{cr} = \frac{0.2220}{D_*^{1.04}} + 0.0550 \cdot (1 - e^{-0.0200 \cdot D_*}) \quad \text{Miedema lower limit} \quad (41)$$

$$\theta_{cr} = \frac{0.2350}{D_*^{1.00}} + 0.0600 \cdot (1 - e^{-0.0250 \cdot D_*}) \quad \text{Miedema upper limit} \quad (42)$$

$$\theta_{cr} = \frac{0.2285}{D_*^{1.02}} + 0.0575 \cdot (1 - e^{-0.0225 \cdot D_*}) \quad \text{Miedema average} \quad (43)$$

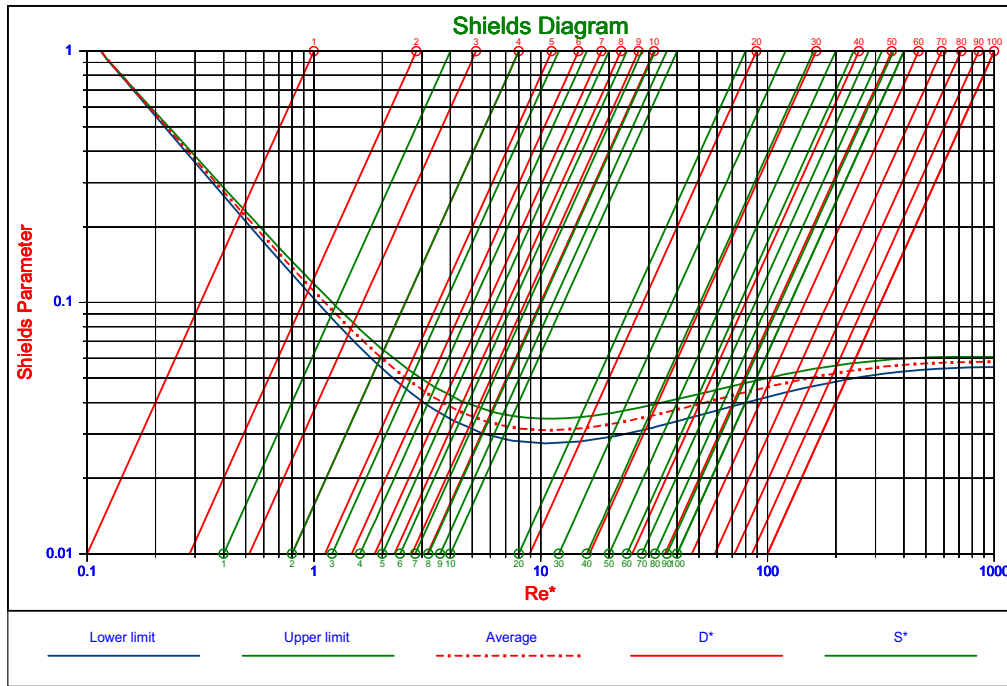


Figure 12. The relation between the boundary Reynolds number, the Bonneville parameter and the Grant and Madsen parameter.

THE HJULSTROM APPROACH

The Hjulstrøm curve is a graph used by hydrologists to determine whether a river will erode, transport or deposit sediment. The graph takes sediment size and channel velocity into account. The x-axis shows the size of the particles in mm. The y-axis shows the velocity of the river in cm/s. The tree lines on the diagram show when different sized particles will be deposited, transported or eroded. The Hjulstrøm curve uses a double logarithmic scale. The curve shows several key ideas about the relationships between erosion, transportation and deposition. The Hjulstrøm curve shows that particles of a size around 1mm require the least energy to erode, as they are sands that do not coagulate. Particles smaller than these fine sands are often clays which require a higher velocity to produce the energy required to split the small clay particles which have coagulated. Larger particles such as pebbles are eroded at higher velocities and very large objects such as boulders require the highest velocities to erode. When the velocity drops below this velocity called the line of critical velocity, particles will be deposited or transported, instead of being eroded, depending on the river's energy. It should be noted however that there is a difference between the line of critical velocity for erosion and deposition. Between the two particles will be transported as bed load. Figures 13 and 14 give examples of Hjulstrøm graphs found on internet.

Threshold of Motion

Grains forming the boundary between a fluid and a sediment possess a finite weight and finite coefficient of friction. When the applied shear stress is low they are not brought into motion. As applied shear stress is increased, a critical shear stress is reached at which grains will begin to move. The value of the critical stress will depend primarily on the size and density of the particles and secondarily on their shape and packing and the cohesive forces acting between particles.

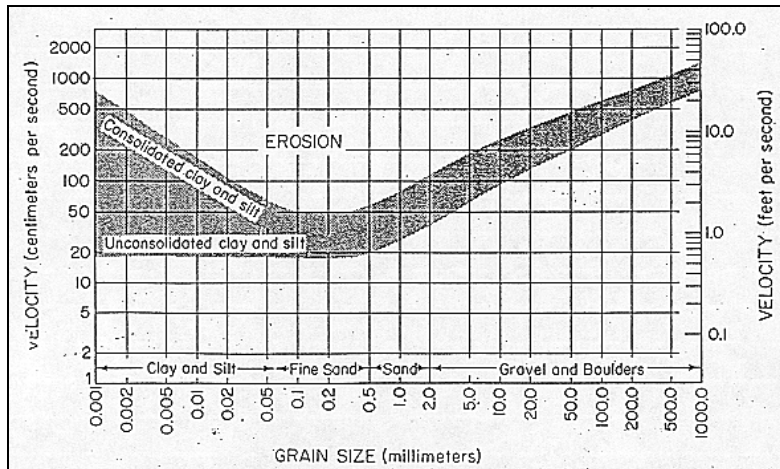


Figure 13. An example of the Hjulström graph.

Once the critical stress is just exceeded, particles will advance in the direction of flow due to irregular jumps or less commonly rolls. This mode of transport is termed the bed load and conceptually can be thought of as being deterministic, that is the behavior of a particle once in motion is dominated by the gravity force. As the stress is further increased, particles will also begin to be suspended in solution and subject to turbulent forces. This mode of transport is termed the suspended load. Due to these two modes of transport there will be a flux of material across a plane perpendicular to the flow. The ultimate goal is to determine this mass flux by integrating the product of the velocity profile and concentration profile.

The Critical Stress

The motion of sediment can be parameterized in a number of ways. The oldest of these is due to Hjulström who summarized observational data in terms of fluid velocity and grain size. There are a number of variants of the Hjulström diagram, using grain diameter as one parameter and some measure of the stress as the other (via the quadratic stress law: u , u_{100} or stress itself: u_*):

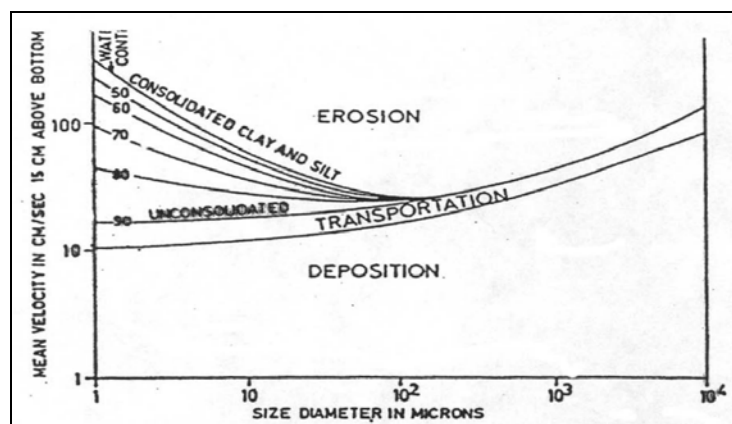


Figure 14. A Hjulström graph showing bed load transportation.

In several of these figures there is an envelope of values for small particles, contrasting unconsolidated and consolidated/cohesive sediment. This reflects the importance of inter particle forces because of the higher ratio of surface area to volume. Sundborg (1956) - added more detail, and dealt with consolidation in fine-grained end. Figure 15 shows the Hjulström curves, normalized for 100cm water depth and compared with Shields curves. In this graph, 3 Shields curves are plotted, first the Soulsby curve, equation 37, second the Miedema curve, equation 42 and third the Brownlie curve, equation 38. Since the Shields curves are derived for non-cohesive soils, they should be more or less horizontal for the very fine particles. The Brownlie and Miedema curves match this, while the Soulsby curve is descending with a decreasing particle diameter. From the analysis in the previous paragraph, this is what should be expected based on equation 20.

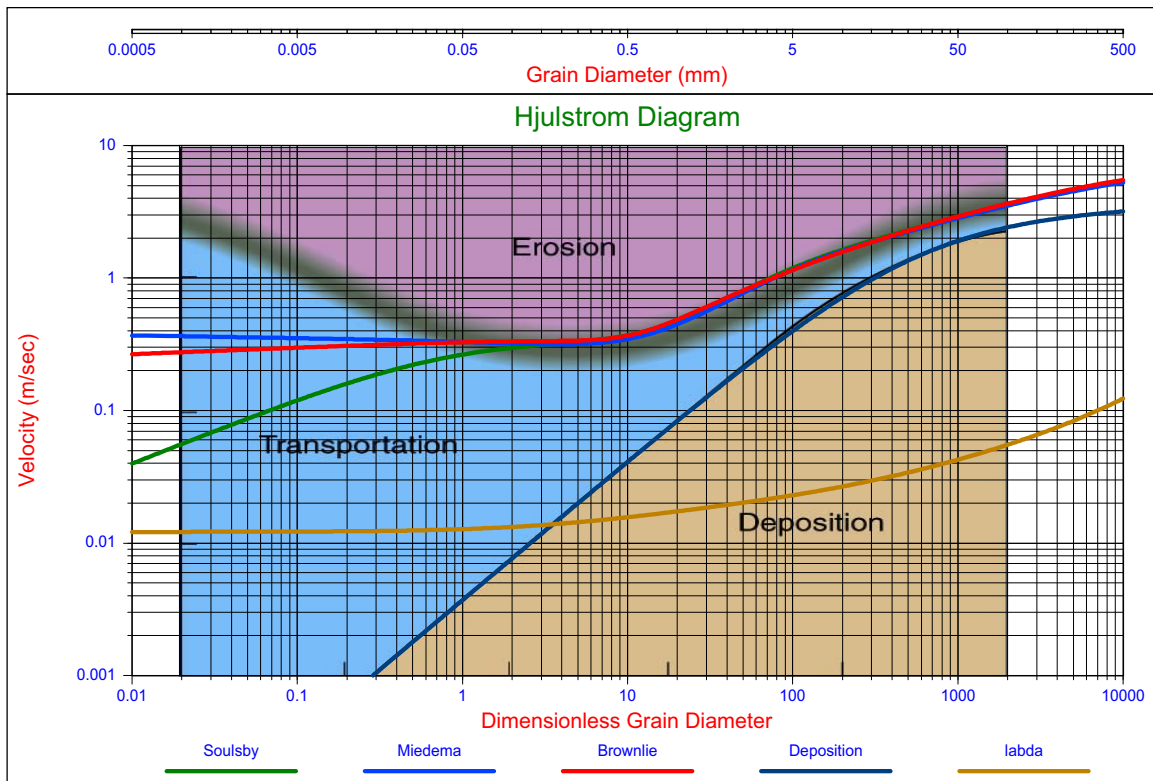


Figure 15. A comparison between the Hjulstrom curve and the Shields curve.

FRICITION COEFFICIENT AND PRESSURE LOSSES WITH HOMOGENEOUS WATER FLOW.

In order to use the above derived theory, a value for the friction coefficient of water flowing above a bed of grains has to be determined. From literature the following relations can be applied. When clear water flows through the pipeline, the pressure loss can be determined with the well known Darcy-Weisbach equation:

$$\Delta p_w = \lambda \cdot \frac{L}{D} \cdot \frac{1}{2} \cdot \rho_w \cdot v^2 \quad (44)$$

The value of the friction factor λ depends on the Reynolds number:

$$\text{Re} = \frac{v \cdot D}{\nu} \quad (45)$$

For laminar flow ($\text{Re} < 2320$) the value of λ can be determined according to Poiseuille:

$$\lambda = \frac{64}{\text{Re}} \quad (46)$$

For turbulent flow ($\text{Re} > 2320$) the value of λ depends not only on the Reynolds number but also on the relative roughness of the pipe ϵ/D . A general implicit equation for λ is the Colebrook-White equation:

$$\lambda = \frac{1}{\left(2 \cdot \log\left(\frac{2.51}{\text{Re} \cdot \sqrt{\lambda}} + \frac{0.27 \cdot \epsilon}{D}\right)\right)^2} \quad (47)$$

For very smooth pipes the value of the relative roughness ϵ/D is almost zero, resulting in the Prandl & von Karman equation:

$$\lambda = \frac{1}{\left(2 \cdot \log\left(\frac{2.51}{\text{Re} \cdot \sqrt{\lambda}}\right)\right)^2} \quad (48)$$

This can be approximated by:

$$\lambda = \frac{0.309}{\left(\log\left(\frac{\text{Re}}{7}\right)\right)^2} \quad (49)$$

At very high Reynolds numbers the value of $2.51/(\text{Re} \cdot \sqrt{\lambda})$ is almost zero, resulting in the Nikuradse equation:

$$\lambda = \frac{1}{\left(2 \cdot \log\left(\frac{0.27 \cdot \epsilon}{D}\right)\right)^2} \quad (50)$$

Because equations 21 and 22 are implicit, for smooth pipes approximation equations can be used. For a Reynolds number between 2320 and 10^5 the Blasius equation gives a good approximation:

$$\lambda = 0.3164 \cdot \left(\frac{1}{\text{Re}}\right)^{0.25} \quad (51)$$

For a Reynolds number in the range of 10^5 to 10^8 the Nikuradse equation gives a good approximation:

$$\lambda = 0.0032 + 0.221 \cdot \left(\frac{1}{\text{Re}}\right)^{0.237} \quad (52)$$

Over the whole range of Reynolds numbers above 2320 the Swamee Jain equation gives a good approximation:

$$\lambda = \frac{1.325}{\left(\ln\left(\frac{d}{3.7 \cdot D} + \frac{5.75}{\text{Re}^{0.9}}\right)\right)^2} = \frac{0.25}{\left(\log\left(\frac{d}{3.7 \cdot D} + \frac{5.75}{\text{Re}^{0.9}}\right)\right)^2} \quad (53)$$

Figure 16 gives the so called Moody diagram, in this case based on the Swamee Jain equation, while Figure 15 also gives a the value of this coefficient based on the relative roughness of the bed for a 100cm deep channel.

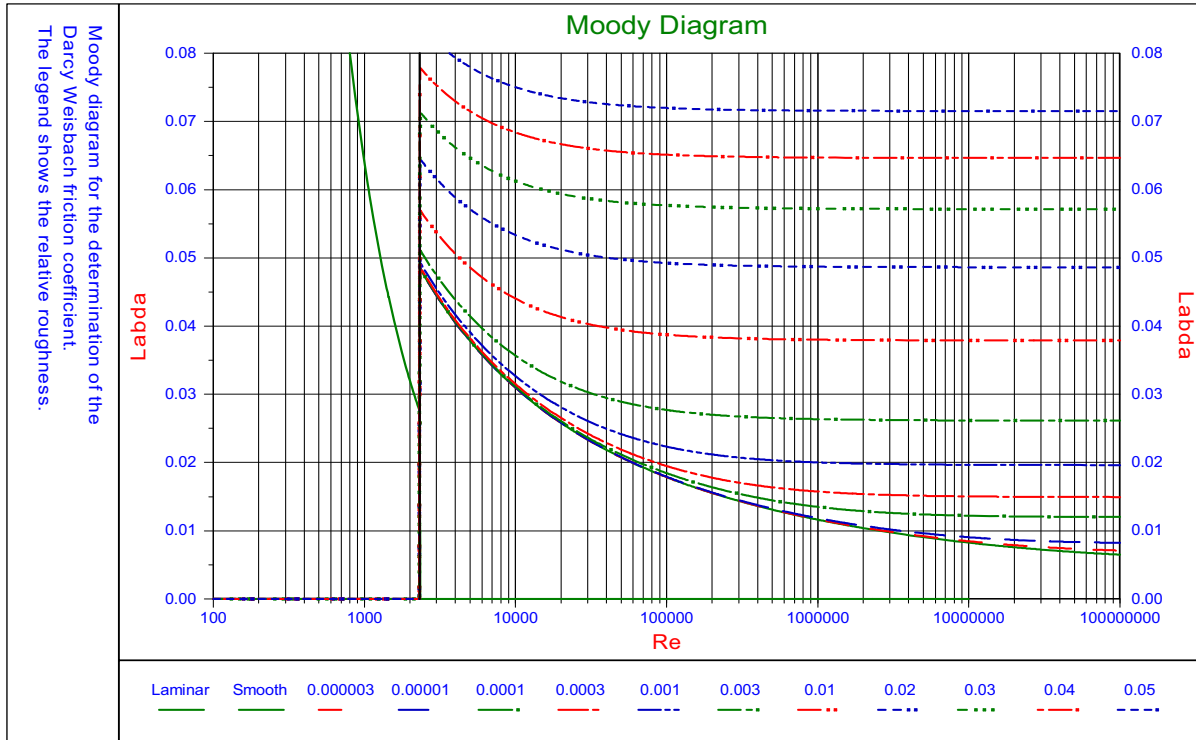


Figure 16. The Moody diagram determined with the Swamee Jain equation.

DETERMINATION OF SCOUR RELATED TO THE TSHD

After discussing the erosion phenomena extensively in the previous paragraphs, it is the question how to apply this in the model for determining the loading process of a TSHD. The first step is to find which particles will not settle due to scour at which average velocity above the sediment in the hopper. The relation between the shear velocity u_* and the average velocity above the bed is U_{cr} :

$$u_*^2 = \frac{\lambda}{8} \cdot U_{cr}^2 \quad (54)$$

Substituting this in equation 12 for the Shields parameter gives:

$$\theta_{cr} = \frac{u_*^2}{R_d \cdot g \cdot d} = \frac{\lambda}{8} \cdot \frac{U_{cr}^2}{R_d \cdot g \cdot d} \quad (55)$$

Re-arranging this gives an equation for the critical average velocity above the bed U_{cr} , that will erode a grain with a diameter d_s :

$$U_{cr} = \sqrt{\frac{8 \cdot \theta_{cr} \cdot R_d \cdot g \cdot d_s}{\lambda}} \quad (56)$$

Equation 56 is almost identical to equation 4 as derived according to the simple Camp (1946) and Huisman (1995) approach. In the same way as equation 5 this can be written as:

$$d_s = \frac{u_*^2}{R_d \cdot g \cdot d} = \frac{\lambda}{8} \cdot \frac{U_{cr}^2}{R_d \cdot g \cdot \theta_{cr}} \quad (57)$$

With a value of $\lambda=0.03$ and $\theta_{cr}=0.05$ equation 57 would be equal to equation 5.

Since the final phase of the hopper loading process is dominated by scour, the above assumption is too simple. Figure 8 shows that the grain sizes we are interested in, from 0.05mm up to 0.5mm, give Shields values θ_{cr} of 0.2 to 0.03 if we use the original Shields curve or one of the approximation curves. The friction coefficient λ , may vary from about 0.01 for fine grains and a smooth bed to 0.03 or higher for a hydraulic rough bed. Figure 15 shows how the value of λ varies as a function of the grain diameter. In the grain size range of interest this λ varies from about 0.01 to 0.02. This results in a range for the ratio between the Shields parameter and the friction coefficient of θ_{cr}/λ of 0.2/0.01 to 0.03/0.02, giving a range of 20 to 1.5. Equation 57 gives a ratio of 1.66 which is in the range and matches with grains of about 0.5 mm, giving an upper limit to the scour velocity.

CONCLUSIONS

The Camp approach matches the Shields approach for one specific case. The Camp approach as used by Huisman (1995) is more a design approach for designing sedimentation tanks. This approach in fact contains some safety in order to be sure there will never be erosion in the sedimentation tank. This approach should not be used for determining erosion in the final stage of the loading of a TSHD.

The Hjulstrøm approach matches the Shields approach for grains from 0.05 mm up to 100 mm (see Figure 15). However a proper scientific and mathematical background of the Hjulstrøm curves was not found. The author had the impression that Hjulstrøm graphs are often copied and redrawn without having a proper background.

The Shields approach is based on a fundamental force and moment equilibrium on grains and has been proven by many scientists in literature. So the Shields approach is the most promising.

Now the question is, which Shields curve to use. Figure 7 shows 7 levels of erosion as defined by Delft Hydraulics (1972). To decide which of these 7 levels is appropriate for the physics of the final stage of hopper loading, these physics should be examined. During this final stage, a high density mixture is flowing over the sediment. Part of the particles in this mixture flow will settle, part will not settle because the settling velocity is too low and part will not settle because of erosion and suspension. This process differs from the erosion process in the fact that there is not water flowing over the sediment, but a high density mixture. In fact the mixture is already saturated with particles and it is much more difficult for a particle to get eroded than in a clean water flow. One could call this hindered erosion. From the experience until now with the erosion model described in this paper (Miedema & van Rhee (2007)) and comparing it with other models, level 7 from Figure 7 should be chosen, this level is achieved by using $\beta=0.475$.

REFERENCES

- Brownlie, W.** (1981), Compilation of alluvial channel data: laboratory and field. Tech. Rep. KH-R-43B, California Institute of Technology, Pasadena, California, USA.
- Camp, T.R.** (1936), "Study of rational design of settling tanks". Sen. Works Journal, Sept. 1936, page 742.
- Camp, T.R.** (1946). "Sedimentation and the design of settling tanks". Trans. ASCE, 895-936.
- Camp, T.R.** (1953), "Studies of sedimentation design". Sen. Ind. Wastes, jan. 1953.
- Clift, R., Grace, J.R. and Weber, M.E.** (1978). Bubbles, Drops and Particles. Academic Press.
- Coulson, J.M., Richardson, J.F., Backhurst, J.R. & Harker, J.H.** (1996). Chemical Engineering. Vol. 1: Fluid Flow, Heat Transfer and Mass Transfer. Butterworth-Heinemann.
- Dobbins, W.E.** (1944), "Effect Of Turbulence On Sedimentation". ASCE Trans. 19443, page 629.
- Grace, J.R.** (1986). Contacting modes and behaviour classification of gas-solid and other two-phase suspensions. Can. J. Chem. Eng., **64**, 353-63.
- Groot, J.M.** (1981), "Rapport Beunbezinking. Boskalis 1981. (From lecture notes of v/d Schrieck 1995).
- Huisman, L.** (1980), "Theory of settling tanks". Delft University of Technology 1980.
- Huisman, L.** (1995), "Sedimentation and Flotation". Lecture Notes, Delft University Of Technology 1973-1995.
- Julien, P.** (1995). Erosion and sedimentation. Cambridge university press, Cambridge.
- Koning, J. de** (1977), "Constant Tonnage Loading System of Trailing Suction Hopper Dredge's". Proc. Modern Dredging, The Hague, The Netherlands 1977.
- Madsen, O.** (1991), Mechanics of cohesionless sediment transport in coastal waters. Proceedings of Coastal Sediments'91. ASCE, Seattle, Washington, ASCE, pp. 15–27.
- Madsen, O., Grant, W.** (1976), Sediment transport in the coastal environment. Tech. Rep. 209, M.I.T., Cambridge, Massachusetts, USA.
- Miedema, S.A.** (1981), "The flow of dredged slurry in and out hoppers and the settlement process in hoppers" ScO/81/105, Delft University of Technology, 1981, 147 pages.
- Miedema, S.A.** (1991), "T.S.H.D.". Computer program for the calculation of hopper loading cycles, Delft, 1991.
- Miedema, S.A. & Vlasblom, W.J.** (1996), "Theory for Hopper Sedimentation". 29th Annual Texas A&M Dredging Seminar. New Orleans, June 1996.
- Miedema, S.A. & Rhee, C. van,** (2007) "A SENSITIVITY ANALYSIS ON THE EFFECTS OF DIMENSIONS AND GEOMETRY OF TRAILING SUCTION HOPPER DREDGES". WODCON ORLANDO, USA, 2007.
- Ooijens, S.** (1999). "Adding Dynamics to the Camp Model for the Calculation of Overflow Losses". Terra et Aqua (76), 12-21.
- Ooijens, S., de Gruijter, A., Nieuwenhuijzen, A. and Vandycke, S.** (2001). "Research on hopper settlement using large-scale modeling". Proceedings CEDA Dredging Days 2001, pp. 1-11.
- van Rhee, C.** (2002). "On the sedimentation process in a Trailing Suction Hopper Dredger". PhD thesis, TU Delft, the Netherlands.
- Richardson, J. and Zaki, W.** (1954). "Sedimentation and Fluidisation: Part I". Transactions of the Institution of Chemical Engineers 32, 35-53.
- Rijn, van, L.C.** (1984), "Sediment Pick up functions", Journal of Hydr. Eng. Vol 110, No. 10, Oct 1984
- Rijn, van, L.C.** (1987), "Mathematical Modelling of Morphological Processes in the case of Suspended Sediment Transport", PhD Thesis, Delft University of Technology, 1987.
- Rijn, van, L. C.** (1993). Principles of sediment transport in rivers, estuaries and coastal seas, Aqua Publications, Oldemarkt, The Netherlands.
- Soulsby, R.** (1987), Calculating bottom orbital velocity beneath waves. Coastal Engineering 11, 371-380.
- Soulsby, R.** (1997), Dynamics of marine sands. Thomas Telford Publications, London, United Kingdom.
- Soulsby, R., Whitehouse, R.** (1997), Threshold of sediment motion in coastal environment. Proceedings Pacific Coasts and Ports 1997 Conference. University of Canterbury, Christchurch, New Zealand, pp. 149–154.
- Terwindt, J. H. J. & Breusers, H. N. C.** (1972), EXPERIMENTS ON THE ORIGIN OF FLASER, LENTICULAR AND SAND-CLAY ALTERNATING BEDDING, **Sedimentology, Volume 19, Issue 1-2, Page 85-98, Sep 1972, doi: 10.1111/j.1365-3091.1972.tb00237.x**
- Vlasblom, W.J. & Miedema, S.A.** (1995), "A theory for determining sedimentation and overflow losses in hoppers". Proc. WODCON XIV, Amsterdam 1995.

- Wallis, G.B.** (1969), One Dimensional Two Phase Flow. McGraw-Hill.
- Wilson, K.C., Addie G.R., Sellgren, A. & Clift, R.** (1997). Slurry Transport Using Centrifugal Pumps. Chapman & Hall, Blackie Academic & Professional.
- Yagi, T.** (1970). "Sedimentation effects of soil in hopper". Proceedings of WODCON 1970.
- Zanke, U.C.E.** (2003), On the influence of turbulence on the initiation of sediment motion, International J. of Sediment Research 18(1), 1-15.

NOMENCLATURE

C_D	Drag coefficient	-
C_L	Lift coefficient	-
d	Grain diameter	m
d_s	Grain diameter (scour)	m
D^*	Bonneville parameter	m
f	Shear force	kN
F_D	Drag force on particle	kN
F_L	Lift force on particle	kN
F_w	Submerged weight of particle	kN
g	Gravitational constant (9.81)	m/sec ²
h	is the overfall height (measured about a distance of 5h upstream from the crest)	m
H	Height of basin	m
k_s	Roughness	m
L	Length of basin	m
N	Normal force	kN
n	Porosity	-
p	Pressure	kPa
Q	Mixture flow	m ³ /sec
R_d	Relative density	-
S^*	Madsen & Grant parameter	-
s_O	Flow velocity in basin	m/sec
s_s	Scour velocity	m/sec
S	Sedimentation flux	
u	Velocity	m/sec
u^*	Shear velocity	m/sec
v	Settling velocity	m/sec
v_O	Hopper load parameter	m/sec
W	Width of basin	m
z	Water depth	m
α	Velocity factor	-
β	Fraction of height particle above the bed	-
λ	Viscous friction coefficient	-
ρ_m	Density of a sand/water mixture	ton/m ³
ρ_q	Density of quarts	ton/m ³
ρ_s	Density of sediment	ton/m ³
ρ_w	Density of water	ton/m ³
τ	Wall shear stress	kPa
θ	Shields parameter (index c, critical Shields parameter)	-
ν	Viscosity	
μ	Friction coefficient	-

